Research in Astronomy and Astrophysics, 22:055019 (6pp), 2022 May https://doi.org/10.1088/1674-4527/ac6310

Detections of Gamma-Rays from Globular Clusters ESO 452-SC11, NGC 6380, Palomar 6 and UKS 1 with Fermi-LAT

Min Yuan, Jiao Zheng, Pengfei Zhang, and Li Zhang
Department of Astronomy, School of Physics and Astronomy, Key Laboratory of Astroparticle Physics of Yunnan Province, Yunnan University, Kunming 650091, China; zhangpengfei@ynu.edu.cn, lizhang@ynu.edu.cn
Received 2022 February 10; revised 2022 March 26; accepted 2022 March 30; published 2022 April 29

Abstract

The events from 157 globular clusters (GCs) are analyzed by using 12 yr long-term Pass 8 data from Fermi Large Area Telescope. Besides the 34 GCs reported in previous literatures, four additional GCs (ESO 452-SC11, NGC 6380, Palomar 6 and UKS 1) in the Milky Way are detected as gamma-ray GC candidates. Especially for UKS 1, these are known as the faintest GCs in long-wavelength bands. Further data analysis has been performed for the four GCs. While no pulsars are determined in radio and/or X-ray wavelengths so far, their gamma-ray pulsation emissions are not found, and no significant gamma-ray flux variability is detected. The numbers of MSPs within the four GCs are estimated based on the assumption that the MSPs within each GC emit similar amounts of gamma-rays. The gamma-ray results reported here could help us better understand the nature of gamma-ray emission origins for GCs.

Key words: (Galaxy:) globular clusters: individual (ESO 452-SC11, NGC 6380, Palomar 6 and UKS 1)

1. Introduction

Globular clusters (GCs) are the most ancient stellar groups with typical ages of 10^{10} yr and dense cores of 100–1000 stars pc^{-3} in the Galaxy. At present, there are 157 GCs detected at radio and/or optical bands in the Milky Way (Harris 1996, 2010 version). Among these GCs, 34 GCs have been detected to emit GeV photons in previous literatures (Abdo et al. 2009, 2010a, 2010b; Kong et al. 2010; Tam et al. 2011; Nolan et al. 2012; Acero et al. 2015; Zhou et al. 2015; Zhang et al. 2016; Lloyd et al. 2018; de Menezes et al. 2019) and the fourth Fermi Large Area Telescope catalog Data Release 2 (4FGL-DR2; Abdollahi et al. 2020; Ballet et al. 2020). For example, gamma-ray emission was detected in 47 Tucanae (NGC 104) for the first time by the Fermi Large Area Telescope (Fermi-LAT) in 2009 (Abdo et al. 2009). Therefore, the search for GeV gamma-ray emissions in GCs plays an important role in understanding the high-energy properties of the GCs.

GCs are known for hosting low-mass X-ray binaries (LMXBs) and populations of millisecond pulsars (MSPs) that arise from binary interactions (Clark 1975; Alpar et al. 1982; Cheng et al. 1986; Liu et al. 2007). On one hand, more than 200 pulsars have been observed in 34 GCs within 20 kpc of the Galactic center, of which more than 90 percent are MSPs.[1] For example, 27 MSPs have been detected in 47 Tucanae (Abdo et al. 2009) and 38 MSPs and 1 normal pulsar in Terzan 5 (Kong et al. 2010). On the other hand, the MSPs have been firmly established as gamma-ray sources (Verbunt et al. 1996; Ibata et al. 2009; Abdo et al. 2013; Espinoza et al. 2013). Moreover, it is generally believed that the gamma-ray emissions from GCs either come from curvature radiation (CR) of relativistic electrons/positrons in magnetospheres of MSPs (CR; Cheng et al. 2010) or are produced by the inverse Compton scattering (IC) between electrons accelerated in the relativistic pulsar wind and background soft photons (IC; Bednarek & Sitarek 2007; Cheng et al. 2010).

In this paper, the gamma-ray emissions from four GCs (ESO 452-SC11, NGC 6380, Palomar 6 and UKS 1) are reported by using 12 yr of survey data with the Fermi-LAT. The spectral energy distributions (SEDs) of these GCs are mainly analyzed and the numbers of MSPs in these GCs are estimated. The remainder of the paper is as follows: In Section 2 we introduce observations and the data analysis procedure. Section 3 presents results of our correlation analysis. We will discuss the results in Section 4.

2. Observations and Data Analysis

After removing 34 gamma-ray GCs reported in previous literatures and 4FGL-DR2, we select 123 from 157 GCs as a sample, and then search for their gamma-ray emissions. In our analysis, the data were collected by Fermi-LAT between 2008 August 8 and 2020 December 29 (Mission Elapsed Time: 239846401 [s]–630892805 [s]). The events within a 15° radius of interest (ROI) centered on the nominal GC target coordinates are considered. The energy range is selected from 100 MeV to 500 GeV, which can effectively suppress the confluence of gamma-ray emission of the Galactic disk. The Fermitools-2.0.0 package[2] is utilized for the newest Pass 8 data that have a high

[1] http://naic.edu/~pfreire/GCpsr.html

[2] https://github.com/fermi-lat/Fermitools-conda/

probability of being photons. According to the Fermi-LAT data analysis threads,[3] event class for the analysis is "Source" class (evclass = 128) and the event type is "FRONT+BACK" (evtype = 3).[4] To eliminate the effects of gamma-rays generated by the interaction between the Earth's atmosphere and cosmic rays, only events with zenith angles <90° and (DATA_QUAL > 0) && (LAT_CONFIG = 1) are selected. The corresponding instrument response function is P8R3_SOURCE_V3.

We use the binned maximum likelihood analysis method and the model files consisting of gamma-ray source population seeded from the 4FGL-DR2 with two diffuse emission backgrounds: Galactic diffuse emission (gll_iem_v07.fit) and extragalactic isotropic diffuse emission (iso_P8R3_SOURCE_V3_v1.txt). In general, the SEDs of the point sources like GC candidates have been fitted using a power law (PL) model. Their differential flux, dN/dE (photon flux per energy bin), of the detected GC is described as PL with formula

$$\frac{dN}{dE} = N_0\left(\frac{E}{E_0}\right)^{-\gamma}. \quad (1)$$

In Equation (1), parameters N_0 and γ are the normalization (gamma-ray flux density) and energy spectral slope, respectively. In the data analysis, for PL, we kept the normalization fluxes and the spectral indices as free parameters. However because of the large populations of MSPs in GCs, their gamma-ray spectral shapes are similar to the pulsars in gamma-ray bands. We also fitted their spectral distributions using a power-law plus exponential cutoff (PLE) model with a formula

$$\frac{dN}{dE} = N_0\left(\frac{E}{E_0}\right)^{-\gamma}\exp\left(-\left(\frac{E}{E_c}\right)^{b}\right). \quad (2)$$

In Equation (2), N_0, γ, b and E_c represent the normalization, low-energy spectral slope, exponential index and cutoff energy, respectively. For PLE, we kept their normalization fluxes, spectral indices and cutoff energies as free parameters. While the population of events coming from the GC candidates is too small to restrict the exponential index, we fixed the exponential index parameter at the value of 1.0 adopted in Abdo et al. (2010b). For the model file, it includes two types of sources that are point-like and spatially extended sources. More information about extended source templates is described detailedly in a Fermi-LAT data analysis thread.[5] In our analysis, the parameters of normalization fluxes and the spectral shapes of all sources within 5° are set free. For the sources located within 5°–10° of ROI, we only set the normalization factors as free, and other parameters are fixed at the values reported in the 4FGL-DR2 catalog.

[3] https://fermi.gsfc.nasa.gov/ssc/data/analysis/scitools/

[4] https://fermi.gsfc.nasa.gov/ssc/data/analysis/scitools/data_preparation.html

[5] https://fermi.gsfc.nasa.gov/ssc/data/access/lat/10yr_catalog/LAT_extended_sources_8years.tgz

In our analysis, for the four GCs, we first generate their 2° × 2° test statistic (TS) maps to verify confidences of the GCs with gamma-ray radiation using the tool *gttsmap*. In order to exclude the influence of a large point-spread function under low energy, we consider the TS maps with the energy region from 400 MeV to 500 GeV (the higher the energy segment, the better the directivity of photons). Then we use the tool *gtlike* to obtain the SEDs. We divided the energy range into 6 equal logarithmically spaced energy bins of four GCs. In this step, all spectral shape parameters are fixed at the best-fit results. The normalizations for the sources within 10° of ROI and the two diffuse backgrounds are set free. We obtained the flux of the target source in each energy bin, by fitting all spectral model components. The results of this analysis are reported in Section 3.

3. Results of the Four GCs

In our analysis, four GC candidates (ESO 452-SC11, NGC 6380, Palomar 6 and UKS 1) are found to emit gamma-rays, but no pulsar has been detected so far in the four GCs. Their fluxes and spectral shape parameters have been determined by employing models with PL and PLE, respectively. Their TS maps and the best-fit spectral shape (i.e., SEDs) are displayed in Figures 1 and 2. The detailed position information and best-fit energy spectral shape parameters for the four GCs are summarized in Tables 1 and 2, respectively.

3.1. Four Potential Gamma-Ray GCs

3.1.1. ESO 452-SC11

ESO 452-SC11 (also known as 1636-283) is a poorly studied object located ∼2 kpc from the Galactic center at low latitude. It was discovered in the ESO/Uppsala B survey (Lauberts et al. 1981). A previous study (Cornish et al. 2006) found that the age of this GC was a possible range between 9 and 16 billion years. ESO 452-SC11 is one of the faintest clusters known in the Milky Way (Harris 1996, and 2010 version), and only has a mass of ∼6800 $M_\odot$ (Simpson et al. 2017), which may make it the lowest mass GC. It is located at a moderate distance of 8.3 kpc away from Sun in the constellation Scorpius.[6] In gamma-ray band, ESO 452-SC11 is found with a TS value of 20 for PL model, corresponding to a detection significance of 4.5σ. The TS value for PLE model is 23 (4.8σ). ESO 452-SC11 is identified as a possible gamma-ray emitter here. Our gamma-ray best-fit position (J2000, the same coordinates following) is R.A. = 249°.91 and decl. = −28°.40 with error of 0°.04. Its nominal position is R.A. = 249°.86 and decl. = −28°.40, and the offset between the two positions is 2′.87. Its tidal radius is 5′.00, and the gamma-ray best-fit position is well within the tidal radius circle of the nominal position. For the models of PL

[6] https://www.skythisweek.info/gc.htm

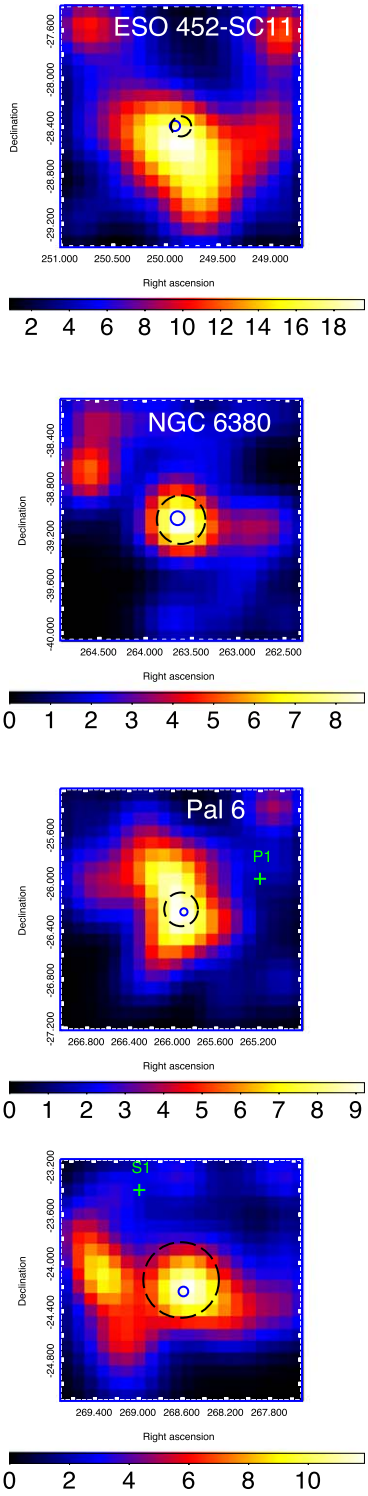

Figure 1. Four TS maps of 2° × 2° ROI with a spatial pixel size of 0.°1 × 0.°1 obtained with events selected over 400 MeV. Their color bars represent TS values scaled with color. The black dashed circles stand for their tidal radii centered coordinates as listed in Harris (1996, 2010 version). The blue solid circles signify the best-fit centroids of the gamma-ray emission with 1σ statistical errors indicating their radii. The maps are smoothed by a Gaussian function with kernel radius of 0.°3.

and PLE, the gamma-ray luminosities of ESO 452-SC11 are derived to be $L^{\rm PL}_{0.1-500\ {\rm GeV}} = (2.12 \pm 0.57) \times 10^{34}$ erg s^{-1} and $L^{\rm PLE}_{0.1-500\ {\rm GeV}} = (1.31 \pm 0.30) \times 10^{34}$ erg s^{-1}, respectively. Its residual TS map and SED are shown in Figures 1 and 2 respectively.

3.1.2. NGC 6380

The GC NGC 6380 (Ton 1), a candidate core-collapsed cluster, is located ∼10.7 kpc from the Sun in the constellation Scorpius. Until now no pulsar has been detected in this cluster. In the data analysis, we fit the events above 100 MeV based on PL and PLE spectral models. The TS value for PL is 15, corresponding to a detection significance of 3.9σ. The TS value for PLE is 26 (5.1σ). Its gamma-ray best-fit position is R.A. = 263.°65, decl. = −39.°06 (with error of 0.°06), which is offset from the nominal position (R.A. = 263.°62, decl. = −39.°07) by 1.′86. Its gamma-ray position is located well within its tidal radius (12.′06) centered at the nominal position. Its gamma-ray luminosities, for two spectral models, are $L^{\rm PL}_{0.1-500\ {\rm GeV}} = (4.26 \pm 1.26) \times 10^{34}$ erg s^{-1} and $L^{\rm PLE}_{0.1-500\ {\rm GeV}} = (3.30 \pm 0.71) \times 10^{34}$ erg s^{-1}, respectively. Its TS map and SED are featured in Figures 1 and 2 respectively.

3.1.3. Palomar 6

Palomar 6 is one of the poorly understood GCs. It is estimated to be ∼12.5 billion years old, located at a distance of 5.8 kpc away from Sun in the constellation Ophiuchus and contains about 500,000 stars. Interestingly in Palomar 6, planetary nebulae were detected (Jacoby et al. 1997). Souza et al. (2021) indicate that Palomar 6 is confined within the central bulge of stars that surround the Galactic center based on the orbital analysis, and it is probably formed in the main-bulge in the early stages of the Milky Way's formation. This is unlike most of the other GCs found in the distant Galactic halo. In gamma-rays, we found evidence for gamma-ray emissions within its tidal radius. We obtain the TS value of 16 for PL model, which corresponds to 4.0σ. For PLE model its TS value is ∼10 (3.2σ). The gamma-ray best-fit position is R.A. = 265.°90 and decl. = −26.°25 (with error of 0.°03) having offset of 2.′01 from its core. Its tidal radius is 8.′36, and the gamma-ray position is well within the tidal radius circle of the nominal position (R.A. = 265.°93, decl. = −26.°23). Its gamma-ray luminosities in two spectral models are $L^{\rm PL}_{0.1-500\ {\rm GeV}} = (1.52 \pm 0.45) \times 10^{34}$ erg s^{-1} and $L^{\rm PLE}_{0.1-500\ {\rm GeV}} = (1.03 \pm 0.34) \times 10^{34}$ erg s^{-1}. In its gamma-ray data analysis, we added a point source (P1 with R.A. = 265.°20 and decl. = −25.°97) marked with a green cross shown in the TS map (Figure 1) to clearly display Palomar 6. Its SED is depicted in Figure 2 (lower left panel).

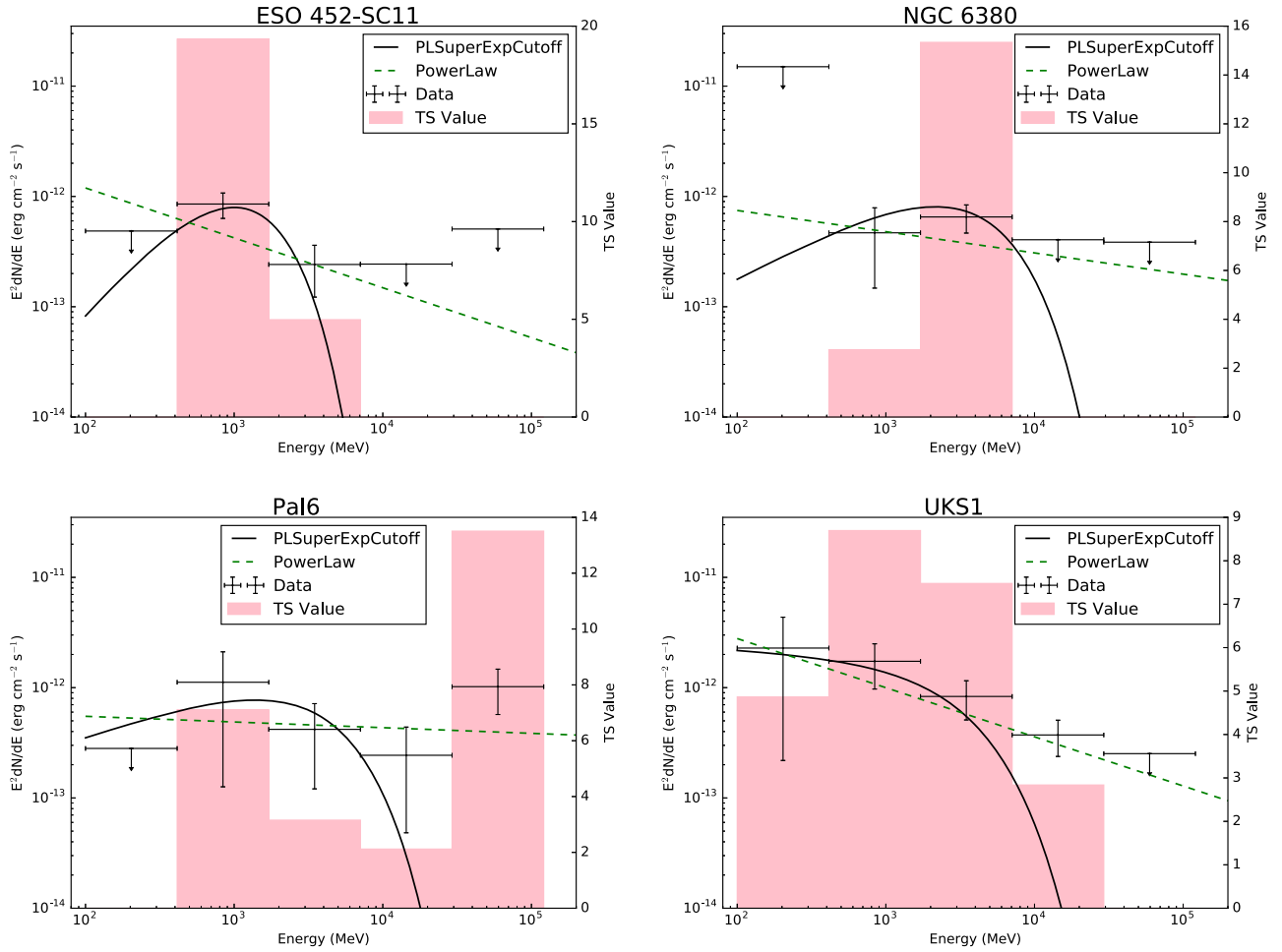

Figure 2. SEDs for ESO 452-SC11, NGC 6380, Palomar 6 and UKS 1. The green dashed lines indicate the best-fit models with spectral function of PL, and the black solid lines represent the best-fit models with spectral function of PLE. We also show the TS values for each data point with pink bars. The detailed information on best-fit model spectral parameters is listed in Table 2.

3.1.4. UKS 1

UKS 1 was discovered by Malkan et al. (1980) and is known as the faintest GC in the Milky Way. It is located at a distance of 7.8 kpc away from the Sun. The events over 100 MeV are fitted using two energy spectral models, and the TS values of two models are ∼16, which translate to 4.0σ. Its nominal position is R.A. = 268.°61 and decl. = −24.°15, and the gamma-ray best-fit position is R.A. = 268.°59 and decl. = −24.°24 (with error of 0.°04). The gamma-ray position is well within the tidal radius of UKS 1 (18.′76) with offset of 5.′82 from its nominal position. Its gamma-ray luminosities for two spectral models are $L^{\rm PL}_{0.1-500\,{\rm GeV}} = (5.20 \pm 1.20) \times 10^{34}$ erg s^{-1} and $L^{\rm PLE}_{0.1-500\ {\rm GeV}} = (4.15 \pm 1.09) \times 10^{34}$ erg s^{-1}. We also added a point source (S1 with R.A. = 268.°99 and decl. = −23.°40) to clearly display UKS 1 in its TS map (shown in the Figure 1) in our data analysis. The other detailed information on best-fit for this GC is listed in Table 2. Its SED is presented in Figure 2.

3.2. Estimated Numbers of MSPs in GCs

The gamma-rays from GCs are generally thought to be dominated by the MSPs contained within such systems. While no pulsar has been detected in those four GCs so far, we estimate the numbers of MSPs in the four GCs based on the assumption that each MSP within a GC emits a similar amount of gamma-rays (Abdo et al. 2009). The numbers of MSPs in GCs are estimated as follows,

$$N_{\rm MSP} = \frac{L_\gamma}{\langle \dot{E} \rangle \langle \eta_\gamma \rangle}, \tag{3}$$

Table 1
Parameters of Gamma-Ray GC Candidates

GC Name	Center of ROI[(1)]		Tidal Radius[(2)]	Position and Error[(3)]			Offset[(4)]	Distance[(5)]
	R.A.	Decl.	(arcmin)	R.A.	Decl.	(radian)	(arcmin)	(kpc)
ESO 452-SC11	249.86	−28.40	5.00	249.91	−28.40	±0.04	2.87	8.3
NGC 6380	263.62	−39.07	12.06	263.65	−39.06	±0.06	1.86	10.7
Palomar 6	265.93	−26.23	8.36	265.90	−26.25	±0.03	2.01	5.8
UKS 1	268.61	−24.15	18.76	268.59	−24.24	±0.04	5.82	7.8

Note. (1) Coordinates derived from Harris (1996, 2010 version) in J2000. (2) The tidal radii for the four GCs. (3) The best-fit positions and 1σ errors derived with tool *gtfindsrc*. (4) The offsets from their cores. (5) The distances from the Sun derived from Harris (1996, 2010 version).

Table 2
Results of Four GCs

GC Name	Spectral Model	TS	Significance $\sqrt{TS}$	Photon Index γ	Photon Index $E_{cut}^{(1)}$	Photon[(2)] (flux)	Energy[(3)] (flux)	Luminosity[(4)]	$N_{MSP}^{(5)}$
ESO 452-SC11	PL	20	4.5	2.45 ± 0.17		5.14 ± 1.37	2.58 ± 0.69	2.12 ± 0.57	15 ± 7
	PLE	23	4.8	0.38 ± 0.97	0.6 ± 0.3	1.77 ± 0.42	1.60 ± 0.37	1.31 ± 0.30	9 ± 4
NGC 6380	PL	15	3.9	2.19 ± 0.64		3.91 ± 1.15	3.12 ± 0.92	4.26 ± 1.26	30 ± 14
	PLE	26	5.1	1.28 ± 1.06	3.0 ± 1.4	2.13 ± 0.45	2.42 ± 0.52	3.30 ± 0.71	23 ± 10
Palomar 6	PL	16	4.0	2.05 ± 0.61		3.26 ± 0.95	3.79 ± 1.11	1.52 ± 0.45	11 ± 5
	PLE	10	3.2	1.54 ± 0.50	2.9 ± 0.5	3.10 ± 1.01	2.57 ± 0.85	1.03 ± 0.34	7 ± 4
UKS 1	PL	16	4.0	2.45 ± 0.58		14.64 ± 3.39	7.17 ± 1.66	5.20 ± 1.20	36 ± 16
	PLE	16	4.0	2.07 ± 0.54	3.0 ± 0.8	11.56 ± 3.02	5.72 ± 1.50	4.15 ± 1.09	29 ± 14

Note. (1) Cutoff energy in unit of GeV. (2) Integrated photon flux in unit of 10^{-9} cm^{-2} s^{-1}. (3) Integrated energy flux in unit of 10^{-12} erg cm^{-2} s^{-1}. (4) Luminosity in unit of 10^{34} erg s^{-1}. (5) The evaluated number of MSPs N_{MSP}.

where $L_\gamma = 4\pi d^2 S$ is the isotropic gamma-ray luminosity of each GC, S is the observed energy flux and d is the distance of the GC from the Sun. In the above expression, $\langle \dot{E} \rangle$ is the average spin-down power of each MSP, and $\langle \eta_\gamma \rangle$ is the estimated average spin-down gamma-ray luminosity conversion efficiency. Here, we use $\langle \dot{E} \rangle = 1.8 \times 10^{34}$ erg s^{-1} and $\langle \eta_\gamma \rangle = 0.08$ as typical values of MSPs in the four GCs, and then estimate the number of MSPs in each GC. These parameters and the number of MSPs estimated for each GC are summarized in Table 2. The estimated numbers of MSPs are higher than the MSP numbers determined in radio and/or X-ray wavelengths, which means that more MSPs will be detected in long-wavelength bands in the future.

4. Conclusions

We have analyzed gamma-rays from 157 GCs cataloged by Harris (1996, 2010 version) in the Milky Way with 12 yr long-term Pass 8 data from Fermi-LAT. Besides the 34 GCs reported in the previous literatures and 4FGL-DR2 (Abdo et al. 2009, 2010a, 2010b; Kong et al. 2010; Tam et al. 2011; Nolan et al. 2012; Acero et al. 2015; Zhou et al. 2015; Zhang et al. 2016; Lloyd et al. 2018; de Menezes et al. 2019; Abdollahi et al. 2020), we have found that four gamma-ray GC candidates (ESO 452-SC11, NGC 6380, Palomar 6 and UKS 1) emit gamma-rays. Their best-fit positions derived in gamma-rays (listed in Table 1) are well within the tidal radius circle centered at their nominal positions (Harris 1996, 2010 version). Note that more data are required to draw definitive conclusions for these four GCs. In the four GCs, Palomar 6 is the closest object at a distance of 5.9 kpc, and NGC 6380 is the most distant at 10.7 kpc. Moreover, UKS 1 is known as the faintest GC in the Milky Way. Palomar 6 is one of the few GCs currently known to contain planetary nebulae. Through analyzing high-resolution spectra obtained with the FLAMES-UVES spectrograph at ESO's Very Large Telescope and photometric data from the Hubble Space Telescope, a photochemo-dynamical analysis of Palomar 6 is conducted in Souza et al. (2021). The parameters of four gamma-ray GCs in terms of gamma-ray luminosity, spectra, number of MSPs and other cluster properties are expressed in Table 2. The residual TS maps and gamma-ray SEDs are featured in Figures 1 and 2. When creating of TS maps for Palomar 6 and UKS 1, we added two point sources P1 and S1 at the positions derived with the Fermi tool *gtfindsrc*, respectively, to show clearly the two GC targets. The additional sources have very little effect on the best-fitting results of Palomar 6 and UKS 1 compared to without them. The data analysis of four GCs indicates that their confidence levels are not very high, which is likely to be their low luminosities of

GeV emission and the strong background emission for the GCs superposed in the Galactic disk.

The gamma-ray emissions observed from GCs are generally believed to be dominated by the MSPs contained within such systems. For the significantly detected GCs, e.g., 47 Tuc and Terzan 5, their SEDs assume the shape of a power-law with an exponential cutoff. For the four GCs, we also use PL and PLE models to fit their events over 100 MeV. The two TS values of spectral models display no obvious difference. In the data reduction, we try to set the parameter b free in Equation (2) for the PLE model. However some errors for this parameter are relatively larger, and this may be caused by the relatively few events from these GCs, which cannot constrain the PLE spectral shape. Therefore $b = 1.0$ for PLE is adopted in our analysis (Abdo et al. 2010b). As shown in Table 2, there are no significant differences between the current four gamma-ray GCs from the results reported in previous literatures (Abdo et al. 2009, 2010a, 2010b; Kong et al. 2010; Tam et al. 2011; Nolan et al. 2012; Acero et al. 2015; Zhou et al. 2015; Zhang et al. 2016; Lloyd et al. 2018; de Menezes et al. 2019; Abdollahi et al. 2020). Although for the four GCs, no pulsar is determined in radio and/or X-ray wavelengths, powerful radio telescopes, like the Five-hundred-meter Aperture Spherical Radio Telescope (FAST; Nan et al. 2011; Li & Pan 2016) and/or the South African MeerKAT facility (Ridolfi et al. 2019) may find some pulsars within these GCs in the future.

The gamma-ray emissions from GCs are thought to come from CR (Cheng et al. 2010) or IC (Bednarek & Sitarek 2007; Cheng et al. 2010). However, it should be pointed out that there are other possible origins of gamma-rays from GCs. In Abramowski et al. (2011), Feng et al. (2012) and Fortes et al. (2020), suspected signs of dark matter were also proposed. These results make GCs potential targets for the indirect detection of dark matter. However in 47 Tucanae, a $\sim$18.4 hr gamma-ray periodic modulation with significance level of $\sim 4.8\sigma$ is reported in Zhang et al. (2020). This scenario may indicate that the gamma-rays from GCs may come from pulsar binary systems (Zhang et al. 2020) and/or dark matter (Abramowski et al. 2011; Feng et al. 2012; Fortes et al. 2020). The origin of gamma-rays from GCs needs more data to draw a definitive research and conclusion. In the future, it is hoped that in-depth observations by these telescopes will provide more observational information on high-energy emission of GCs, but these topics are beyond the scope of this work.

Acknowledgments

We thank the anonymous referee for his/her comments that helped improve this work's results. This work is supported in part by the National Key R&D Program of China under Grant No. 2018YFA0404204, the National Natural Science Foundation of China (NSFC, Grant No. 12163006), the Basic Research Program of Yunnan Province No. 202 101AT070394, and the Joint Foundation of Department of Science and Technology of Yunnan Province and Yunnan University (2018FY001 (−003)).

References

Abdo, A. A., Ackermann, M., Ajello, M., et al. 2009, Sci, 325, 845
Abdo, A. A., Ackermann, M., Ajello, M., et al. 2010a, ApJS, 188, 405
Abdo, A. A., Ackermann, M., Ajello, M., et al. 2010b, A&A, 524, A75
Abdo, A. A., Ajello, M., Allafort, A., et al. 2013, ApJS, 208, 17
Abdollahi, S., Acero, F., Ackermann, M., et al. 2020, ApJS, 247, 33
Abramowski, A., Acero, F., Aharonian, F., et al. 2011, ApJ, 735, 12
Acero, F., Ackermann, M., Ajello, M., et al. 2015, ApJS, 218, 23
Alpar, M. A., Cheng, A. F., Ruderman, M. A., & Shaham, J. 1982, Natur, 300, 728
Ballet, J., Burnett, T. H., Digel, S. W., & Lott, B. 2020, arXiv:2005.11208
Bednarek, W., & Sitarek, J. 2007, MNRAS, 377, 920
Cheng, K. S., Chernyshov, D. O., Dogiel, V. A., Hui, C. Y., & Kong, A. K. H. 2010, ApJ, 723, 1219
Cheng, K. S., Ho, C., & Ruderman, M. 1986, ApJ, 300, 500
Clark, G. W. 1975, ApJL, 199, L143
Cornish, A. S. M., Phelps, R. L., Briley, M. M., & Friel, E. D. 2006, AJ, 131, 2543
de Menezes, R., Cafardo, F., & Nemmen, R. 2019, MNRAS, 486, 851
Espinoza, C. M., Guillemot, L., Çelik, Ö., et al. 2013, MNRAS, 430, 571
Feng, L., Yuan, Q., Yin, P.-F., Bi, X.-J., & Li, M. 2012, JCAP, 2012, 030
Fortes, E. C., Miranda, O. D., Stecker, F. W., & Wuensche, C. A. 2020, JCAP, 2020, 010
Harris, W. E. 1996, AJ, 112, 1487
Ibata, R., Bellazzini, M., Chapman, S. C., et al. 2009, ApJL, 699, L169
Jacoby, G. H., Morse, J. A., Fullton, L. K., Kwitter, K. B., & Henry, R. B. C. 1997, AJ, 114, 2611
Kong, A. K. H., Hui, C. Y., & Cheng, K. S. 2010, ApJL, 712, L36
Lauberts, A., Holmberg, E. B., Schuster, H. E., & West, R. M. 1981, A&AS, 43, 307
Li, D., & Pan, Z. 2016, RaSc, 51, 1060
Liu, Q. Z., van Paradijs, J., & van den Heuvel, E. P. J. 2007, A&A, 469, 807
Lloyd, S. J., Chadwick, P. M., & Brown, A. M. 2018, MNRAS, 480, 4782
Malkan, M., Kleinmann, D. E., & Apt, J. 1980, ApJ, 237, 432
Nan, R., Li, D., Jin, C., et al. 2011, IJMPD, 20, 989
Nolan, P. L., Abdo, A. A., Ackermann, M., et al. 2012, ApJS, 199, 31
Ridolfi, A., Freire, P. C. C., Gupta, Y., & Ransom, S. M. 2019, MNRAS, 490, 3860
Simpson, J. D., De Silva, G., Martell, S. L., Navin, C. A., & Zucker, D. B. 2017, MNRAS, 472, 2856
Souza, S. O., Valentini, M., Barbuy, B., et al. 2021, A&A, 656, A78
Tam, P. H. T., Kong, A. K. H., Hui, C. Y., et al. 2011, ApJ, 729, 90
Verbunt, F., Kuiper, L., Belloni, T., et al. 1996, A&A, 311, L9
Zhang, P. F., Xin, Y. L., Fu, L., et al. 2016, MNRAS, 459, 99
Zhang, P.-F., Zhou, J.-N., Yan, D.-H., et al. 2020, ApJL, 904, L29
Zhou, J. N., Zhang, P. F., Huang, X. Y., et al. 2015, MNRAS, 448, 3215